CELL-INTEGRATED SENSING FUNCTIONALITIES FOR SMART BATTERY SYSTEMS WITH IMPROVED PERFORMANCE AND SAFETY

GA 957273

D 2.2- DEVELOPMENT OF PRINTED ELECTRODES ON CELL COMPONENTS (SEPARATOR).

LC-BAT-13-2020 - Sensing functionalities for smart battery cell chemistries

Deliverable No.	2.2	
Related WP	2	
Deliverable Title	Development of printed electrodes on cell components (separator)	
Deliverable Date	25-05-2022	
Deliverable Type	REPORT	
Dissemination level	Public (PU)	
Written By	Hossein Beydaghi (BDM) Sebastiano Bellani (BDM)	27-04-2022 27-04-2022
Checked by	Francesco Bonaccorso (BDM) Silvia Bodoardo (POL)	04-05-2022 05-05-2022
Reviewed by	Iñigo Gandiaga (IKE) Rahul Gopalakrishnan (ABEE)	06-05-2022 23-05-2022
Approved by	Iñigo Gandiaga (IKE)	25-05-2022
Status	Final	25-05-2022

Summary

The deliverable D.2.2 "Report on development of printed electrodes on cell components and their performance evaluation" summarizes the activities related to the Task 2.2 of the WP2. The main objective is to design and realize the novel sensing technology consisting of printed reference electrodes enabling in situ Electrochemical Impedance Spectroscopy (EIS), reliable in operando measurement of the electrolyte conductivity and in addition to proposal targets, accurate monitoring of cathode and anode potentials during the cell operation. More specifically, Task 2.2 is focused on the print of the produced inks and pastes in Task 2.1 on the separator (in particular, Celgard 2500).

The inks/pastes, containing the materials selected in Task 2.1's activities, have been formulated to find the optimum ratio of lithium iron phosphate (LFP) and lithium titanate (LTO) as the active materials, polyvinylidene difluoride (PVDF) as the binder and carbon black (CB) and single-/few-layer graphene (SLG/FLG) as the conductive materials. Various printing techniques, including doctor blade coating, screen printing and ink-jet printing have been evaluated for the deposition of the produced inks and pastes in Task 2.1 on different substrates (i.e., Celgard 2500, Al and Cu foil), on which we performed preliminary characterizations.

The acquired data showed that the optimized pastes including 25 wt% of active materials (LFP or LTO) achieved the best results in terms of electrical conductivity and electrochemical properties. Resistivity on the order of 0.06 Ω·cm has been achieved for the optimum printed reference electrodes including 25 wt% of active materials. The key fact of this result is linked to the possibility to use an electrical equivalent circuit established for mesh-like reference electrodes, enabling the calculation of the impedance contribution of our reference in the whole cell. The specific capacities of the selected reference electrodes, including 25 wt% of active materials approach the expected theoretical capacities, indicating an optimal use of the active materials. Based on the outcome of these tasks, our printed reference electrodes are currently used for the SENSIBAT project activities related to Tasks 2.3 and 2.4. Our printed reference electrodes will be in-depth characterized in terms of electrochemical properties, aiming at obtaining artifact-free EIS cathode/anode potential monitoring measurements.

This deliverable and the related task do not include any deviation from the objectives and timings planned in the Grant Agreement of the SENSIBAT project.

Table of Contents

List of Figures

List of Tables

Abbreviations

Symbol / Abbreviation	
AFM	*Atomic force microscopy*
CB	*Carbon black*
EIS	*Electrochemical Impedance Spectroscopy*
GCD	Galvanostatic charge/discharge
LFP	*Lithium iron phosphate ($LiFePO_4$)*
LTO	*Lithium titanate ($Li_4Ti_5O_{12}$)*
NMP	*N-Methyl-2-pyrrolidone*
OCP	Open circuit potential
PET	Polyethylene terephthalate
PVDF	*Polyvinylidene difluoride*
RMS	*Root Mean Square*
SEM	*Scanning electron microscopy*
SLG/FLG	*Single-/few-layer graphene*
TGA	Thermogravimetric analysis
WJM	*Wet-jet milling*

1 Introduction

WP2 relates to a sensing technology consisting of printed reference electrodes that enable *in situ* Electrochemical Impedance Spectroscopy (EIS) and reliable *in operando* measurements of the electrolyte conductivity and its change during the cell operation. In addition, the monitoring of the cathode/anode potentials during battery operation has been also considered as an extra functionality for SENSIBAT printed reference electrodes to mitigate overcharging effects leading to degradation issues (electrolyte decomposition and electrode oxidation). Following the submission of deliverable D2.1 related to the activities of Task 2.1, BDM printed sensing reference electrodes onto porous battery separators, namely Celgard 2500 (Task 2.2). The D2.2 report summarizes the activities related to the Task 2.2 of WP2 carried out by BDM (WP Leader) with the support of POL. More in detail, this task concerned the development of printed electrodes on a separator (Celgard 2500).

Meanwhile, flexible, flat electrical connections to the reference electrodes were designed (Task 2.3), permitting preliminary electrochemical characterizations of our sensing electrodes in pouch cell configurations (Tasks 2.4, 2.5). In fact, the activities of Task 2.4 and Task 2.5 were anticipated in Task 2.2 to validate our reference electrode formulations, while checking processability of the electrode inks through printing techniques. The outcomes of Task 2.4 and Task 2.5 were therefore considered to refine the technology developed in Tasks 2.2.

POL and BDM characterized the samples through electrical and electrochemical techniques, including Li plating/stripping test, open circuit potential (OCP) monitoring, galvanostatic charge/discharge (GCD) measurements, and EIS measurements. Thus, this report includes additional preliminary electrochemical characterizations of the printed reference electrodes. These characterizations are currently continued in the activities related to subsequent project's tasks.

2 Printing process

2.1 Formulation of printable inks and pastes

BDM produced various reference electrodes with different formulations, including active materials, *i.e.*, lithium iron phosphate *(*LFP) [1] and lithium titanate (LTO) [2], binder, *i.e.*, polyvinylidene difluoride (PVDF). and conductive materials, *i.e.*, carbon black (CB) and wet-jet milling (WJM)-produced single-/few-layer graphene (SLG/FLG) [3, 4] (see **Table 1**). The screening of these formulations enabled to retrieve the optimal content of each component, in terms of electrical conductivity and the processing/printability of the pastes. According to the activities of Task 2.1, the CB nanoparticles act as effective spacers between SLF/FLG flakes, avoiding the re-stacking of the latter, while guarantying their electrical connection [5]. The reference electrode pastes were formulated by modifying protocols reported in previous literature [6], aiming at optimizing the ratio between active component (LFP or LTO), and the electrically conductive component (SLG/FLG) of the printed reference electrode. This allowed to formulate inks/pastes to be printed onto the chosen separator but also to reach a proper electron conductivity to prepare the reference electrode before its use in the cell. This was achieved by incorporating WJM-produced SLG/FLG. Thus, the produced pastes were printed on a glass substrate through a doctor blade thin film applicator for a preliminary electrical characterization.

Table 1. Electrical performances of the produced reference electrode.

Product name	Component content (wt%)				Resistivity (Ω·cm)
	Active material (LFP/LTO)	PVDF	FLG/SLG	CB	
LFP-A	25	25	25	25	0.060
LFP-B	50	25	12.5	12.5	0.065
LFP-C	16.6	50	16.6	16.6	0.055
LFP-D	65	10	12.5	12.5	0.088
LFP-E	80	5	7.5	7.5	0.250
LFP-F	80	10	5	5	0.371
LTO-A	25	25	25	25	0.066
LTO -B	50	25	12.5	12.5	0.109
LTO -C	16.6	50	16.6	16.6	0.060
LTO -D	65	10	12.5	12.5	0.256
LTO -E	80	5	7.5	7.5	1.370
LTO -F	80	10	5	5	1.560

As shown in **Table 1**, the (volumetric) resistivities of the produced reference electrodes can reach values as low as 0.06 Ω·cm. These results are important in the context of the ongoing activities related to Task 2.4 and 2.5. In fact, the electrodes have resistivity values that from one hand are high enough to act as reference electrode,

and on the other hand low enough to sustain the lithiation process, which is needed to stabilize its potential. It is so possible to use a mesh-like impedance modelling for the developed reference electrodes during EIS analyses. By increasing the active materials loading up to 80 wt%, the resistivity of the films significantly increases, making more difficult the initial stabilization process. Therefore, the reference samples with lower resistivity (LFP-A, LFP-D, LTO-A and LTO-B) were selected for the subsequent activities of the project. BDM upscaled the production of the printable pastes used for the fabrication of the reference electrodes. The production capacity on the BDM pilot line, based on planetary mixers, is on the order of 2 kg/day.

2.2 Printing of produced inks and pastes on the separator

The produced inks/pastes were preliminary printed on flexible substrates, including plastics and paperboards to check the printability of the reference pastes. Various printing methods are available to accomplish manufacturing procedures of reference electrodes [7]. Therefore, ink-jet printing, Doctor blade and screen-printing techniques were investigated for the realization of our printed reference electrodes. Both Doctor blade and screen printing resulted in homogeneous films/patterns using a single-pass deposition protocol. On the contrary, ink-jet printing led to process criticalities because multiple printing passes were needed to obtain the targeted thickness (*e.g.*, between 1-10 µm), and nozzle clogging was occasionally observed. More in detail, Doctor blade coating represents a widely used technique to produce thin films with well-defined thicknesses on large-area surfaces, without requiring accurate control of rheological properties (*e.g.*, thixotropy), which are instead requested by screen printing. It also has low paste losses, typically lower than 5% [8]. Therefore, Doctor blade coating was typically preferred for the activity carried out to accomplish the Task 2.2. The technique works by placing a sharp blade at a fixed distance from the surface that needs to be covered. The pastes are then placed on the substrate beyond the blade. When a constant relative movement is established between the blade and the substrate, the pastes spread on the substrate to form a thin film after drying. Screen printing is the process of transferring a stenciled design onto a flat substrate using an intended ink [9]. The basic method of producing reference electrodes by screen printing method involves pushing ink through a screen over a stencil to create an imprint of the design on the substrate. For both the two printing methods, BDM upscaled the printed reference electrode area up to 350mm(L) x 180mm(W)/pass through (semi)automized Doctor blade film applicator and screen printer (**Figure 1**).

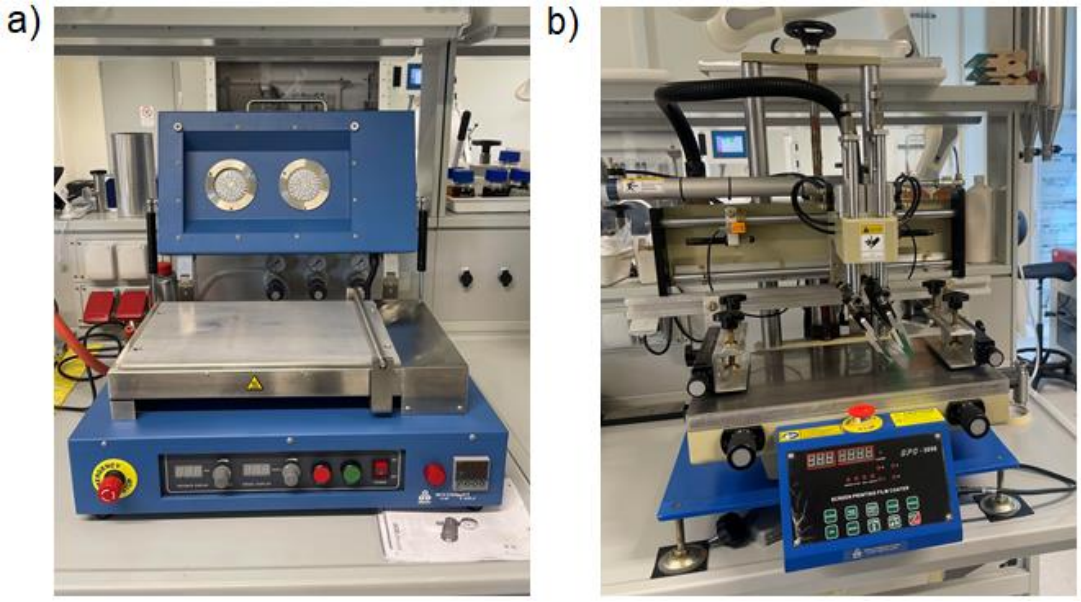

Figure 1. a) Doctor blade film applicator and b) screen printer used by BDM for the Task 2.2.

In order to investigate the performance of the printed reference electrodes, BDM printed reference electrode pastes, based both on LTO and on LFP as the active materials, on: 1) glass substrate for electrical conductivity measurements (**Figure 2a**); 2) Al foil (for LFP-based product) and Cu foil (for LTO-based product) substrates for the electrochemical characterizations of the resulting electrode in coin cell configuration (**Figure 2b**), and 3) battery porous separators (namely Celgard 2500) for the electrochemical characterization of pouch cell in a three-electrode cell configuration using our printed reference electrodes (**Figure 2c**). As previously commented in Deliverable D2.1, the printed reference electrodes on the battery separator (Celgard 2500) have shown satisfactory compatibility with 1 M commercial $LiPF_6$ EC:DEC (1:1) electrolyte used for the project.

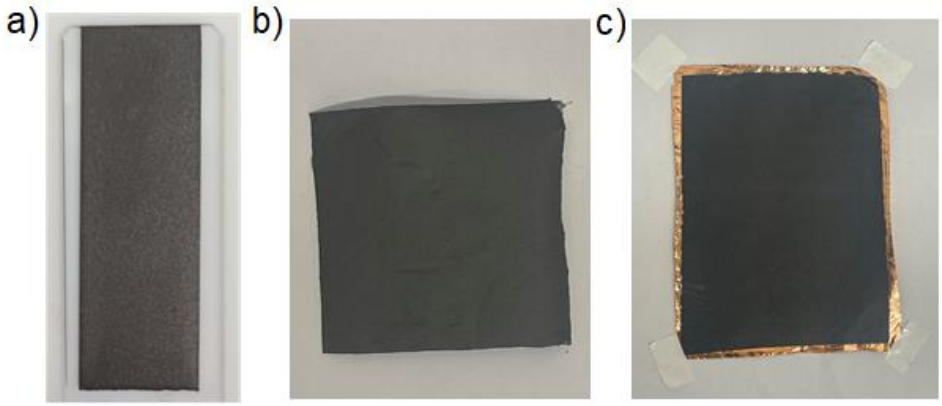

Figure 2. Representative LTO-A reference electrode deposited on a) glass, b) Celgard 2500 and c) Cu foil substrates.

The influence of the active materials volume fraction, as well as their shape and spatial arrangement, on the electrical, mechanical, thermal, and morphological properties of the reference electrodes have been carefully investigated through electrical (four-probe conductivity), mechanical (tensile test), thermogravimetric analysis (TGA), atomic force microscopy microscopic (AFM) and scanning electrode microscopy (SEM) measurements. The outcomes of four-probe conductivity measurements have been already discussed in section 2.1 (see **Table 1).** The mechanical properties of the films deposited on PET substrates were evaluated by measuring the electrical resistance as a function of the tensile strain. All the produced films withstand tensile strain significantly superior to 20%. In addition, TGA curves of the dried printed films demonstrated that they withstand the typical operating temperature of Li-ion batteries (*i.e.*, -20 °C-60 °C as defined in the project requirements deliverable D1.1). The morphologies of the reference electrodes printed by doctor blade on glass substrates were investigated through AFM and SEM measurements. **Figure 3a** shows the AMF images of the LFP-A reference electrode, which exhibit a root mean square (RMS) roughness of 611 nm.

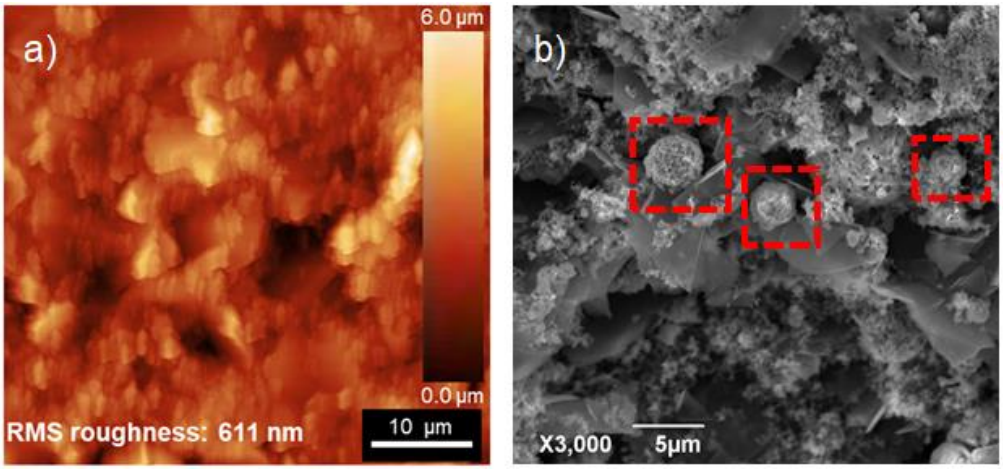

Figure 3. a) AFM and b) SEM images of the LFP-A reference electrode deposited on glass substrates.

The SEM image of the LFP-A surface (**Figure 3b**) evidences a homogeneous dispersion of the LFP particles and SLG/FLG flakes within the electrode structure, without showing any relevant material aggregation. The CB nanoparticles also interconnect SLG/FLG flakes, creating a well-connected conductive network surrounding the active material (LFP) particles. Flat-flex wiring, used to electrically connect our reference electrode to an external pin, were preliminary investigated to evaluate the compatibility of the polymeric binders used in the printed reference electrodes with the electrical connection proposed for the subsequent cell assembly (see additional details in Deliverable D2.1 and next Deliverable D2.3).

3 Results

3.1 GCD characterization of the printed reference electrodes

Electrochemical cycling tests were performed in order to evaluate the influence of our printed reference electrodes, fully covering one Celgard 2500 separator of a prototypical battery (cathode: NMC 622 with a theoretical capacity of 2.7 mAh cm^{-2}; anode: graphite, as defined by the project). GCD measurements of battery pouch cells with and without LFP-A reference electrode were performed at C-rates of C/10 and C/5. A scheme of the two investigated battery configurations is shown in **Figure 4**. Two uncoated Celgard 2500 were used as separators in the reference cell (**Figure 4a**), while one reference electrode-coated Celgard 2500 plus an uncoated Celgard formed the separator in reference electrode-integrating cells (**Figure 4b**).

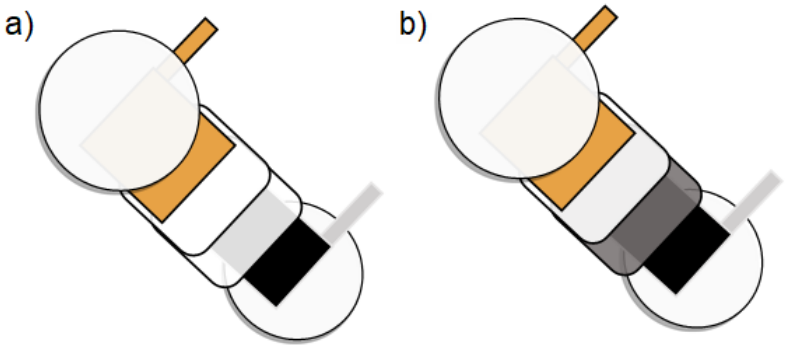

Figure 4. Sketch of batteries using: a) 2 uncoated Celgard 2500 and b) LFP-A-coated Celgard 2500 (grey) plus an additional uncoated Celgard 2500.

The cells were cycled in the potential window from 3.0 V to 4.2 V (**Figure 5**), in agreement with the specifications of the cell electrodes. The cyclability of both configurations was satisfactory, regardless of the presence of the printed reference electrodes. This means that the printed reference electrode does not block the lithium-ion conduction in the electrolyte. The only difference between the two profiles is the shortening of charge/discharge times for the cell including LFP-A coated Celgard 2500. This effect may be associated to the additional impedance contribution of our reference electrode, whose study is on-going in Task 2.4. Overall, these results were positively evaluated, since our reference electrode configuration covered completely one surface of a Celgard 2500, reflecting the worst-case scenario. The use of a separator partially covered by the designed printed reference electrode, as well as the reduction of the thickness of the reference electrode, are expected to improve the performance shown by these preliminary tests, as currently investigated in Task 2.4. Nevertheless, the fully coated separator configuration was preliminarily investigated since it also enables the modelling of our reference electrode through an equivalent electrical circuit previously proposed for mesh-type reference electrodes. The application of a mesh-like model for our reference electrode is possible under the assumption that the resistivity of the reference electrode is significantly lower than the one of the electrolyte. As previously discussed, this hypothesis is verified for the selected printed reference electrodes. the expected advantages of our printed reference electrodes compared to mesh-type reference electrodes already reported in the literature are two-fold. First, the porosity of our reference electrodes intrinsically eliminates the bulky structure of mesh wires, the latter affecting the Li-ion transport through the cell and causing the so-called ion blocking effect, which is the cause of cell performance degradation [10]. Secondly, the flat nature of our reference cell eliminates excessive compression stresses on the cell components, as occurs in the case of mesh-type reference electrodes [11].

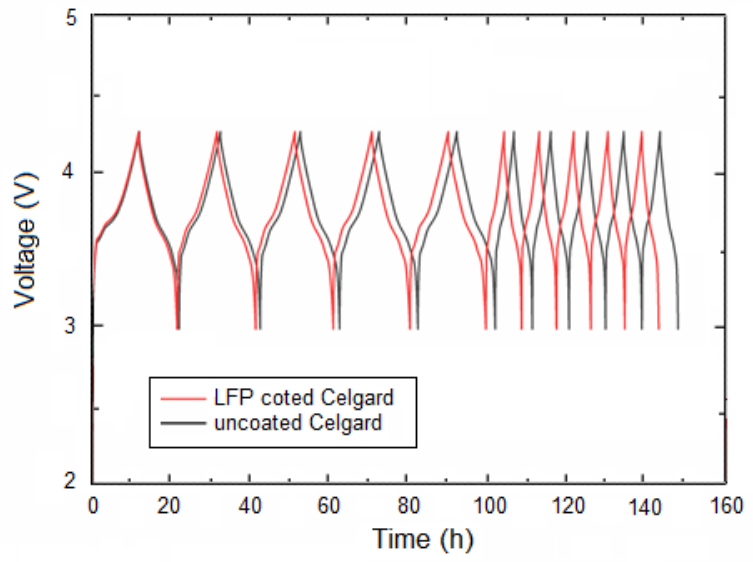

Figure 5. GCD curves measured for the pouch cells including LFP-A-coated Celgard 2500 plus an uncoated Celgard 2500 (reference cell) and 2 uncoated Celgard 2500, respectively, at different current densities.

3.2 Li plating/stripping characterization of the printed reference electrodes

The effect of the presence of the designed reference electrodes on battery separator was further evaluated through the Li plating/stripping test at the current densities of 0.1, 0.5 and 1 mA cm^{-2} using Li/Li symmetric cells (**Figure 6**). The basic principle of this test is assessing the needed potential for alternatively Li plating and stripping on Li electrodes [12].

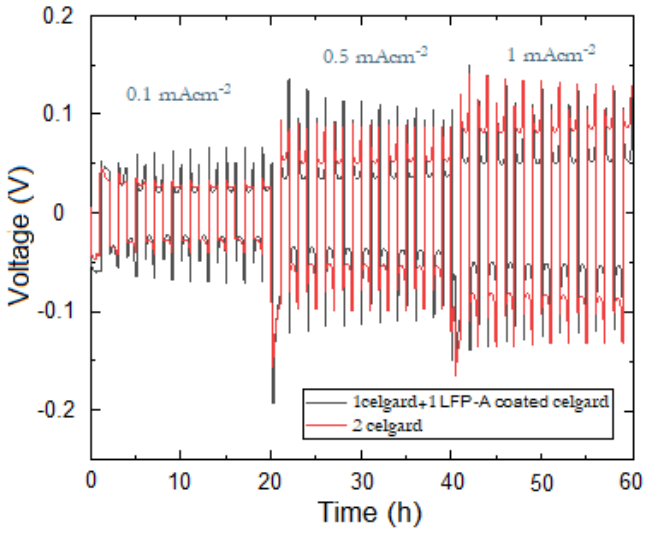

Figure 6. Galvanostatic Li plating/stripping cycling profiles for the pouch cells including LFP-A-coated Celgard 2500 plus an uncoated Celgard 2500 and 2 uncoated Celgard 2500, respectively, at different current densities.

A comparison of the plating/stripping profiles at different currents for differently coated separators could give information about the opposed resistance by the separator to the lithium migration from anode to cathode. The cells with and without the printed reference electrodes have shown comparable reversibility and plating/stripping overpotentials, associated to the porosity and electrolyte wettability of the LFP-A reference electrode coating the Celgard 2500 separator.

3.3 Capacity analysis

The specific capacity of the printed reference electrodes was investigated in both coin cell and pouch cell configurations. To investigate the capacity of the produced reference electrodes in coin cell configuration, we deposited our produced reference electrodes on Al foil (for LFP-based electrodes) and Cu foil (for LTO-based electrodes) substrates by Doctor blade method. **Figure 7** shows that the specific gravimetric capacities of LFP-A, LFP-D, LTO-A and LTO-B samples in coin cell configurations are 161, 150, 144 and 129 mAh g^{-1}, respectively. These results confirm that the specific capacities of the produced reference electrodes are close to the theoretical capacity expected for our active materials (170 mAh g^{-1} for LFP and 175 mAh g^{-1} for LTO) [13, 14]. The obtained results confirm that both LFP and LTO-based printed reference electrodes optimally utilize the active materials, which is the trivial requirement for the practical implementation as reference electrodes.

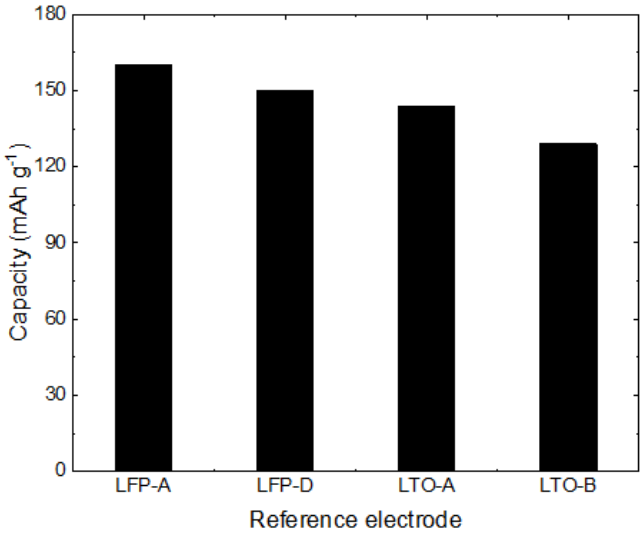

Figure 7. Gravimetric specific capacity of the investigated printed reference electrodes in coin cell configurations.

Figure 8a and **8b** show the specific areal capacity of the LFP/LTO-A produced reference electrodes in pouch cell configuration. As for the coin cell configurations, both LFP-A and LTO-A reference electrodes have shown an areal capacity near the expected theoretical ones. The GCD curves of the reference electrode (**Figure 8c** and **8d)** shows that both LFP and LTO undergo two-phase reactions upon intercalation and deintercalation with Li-ion inside the active materials of the electrode, resulting in stable and constant equilibrium potential. However, the potential plateau of LTO-based printed reference electrodes is flatter than LFP-based electrodes, which makes LTO-based electrodes a better option for electrode potential monitoring.

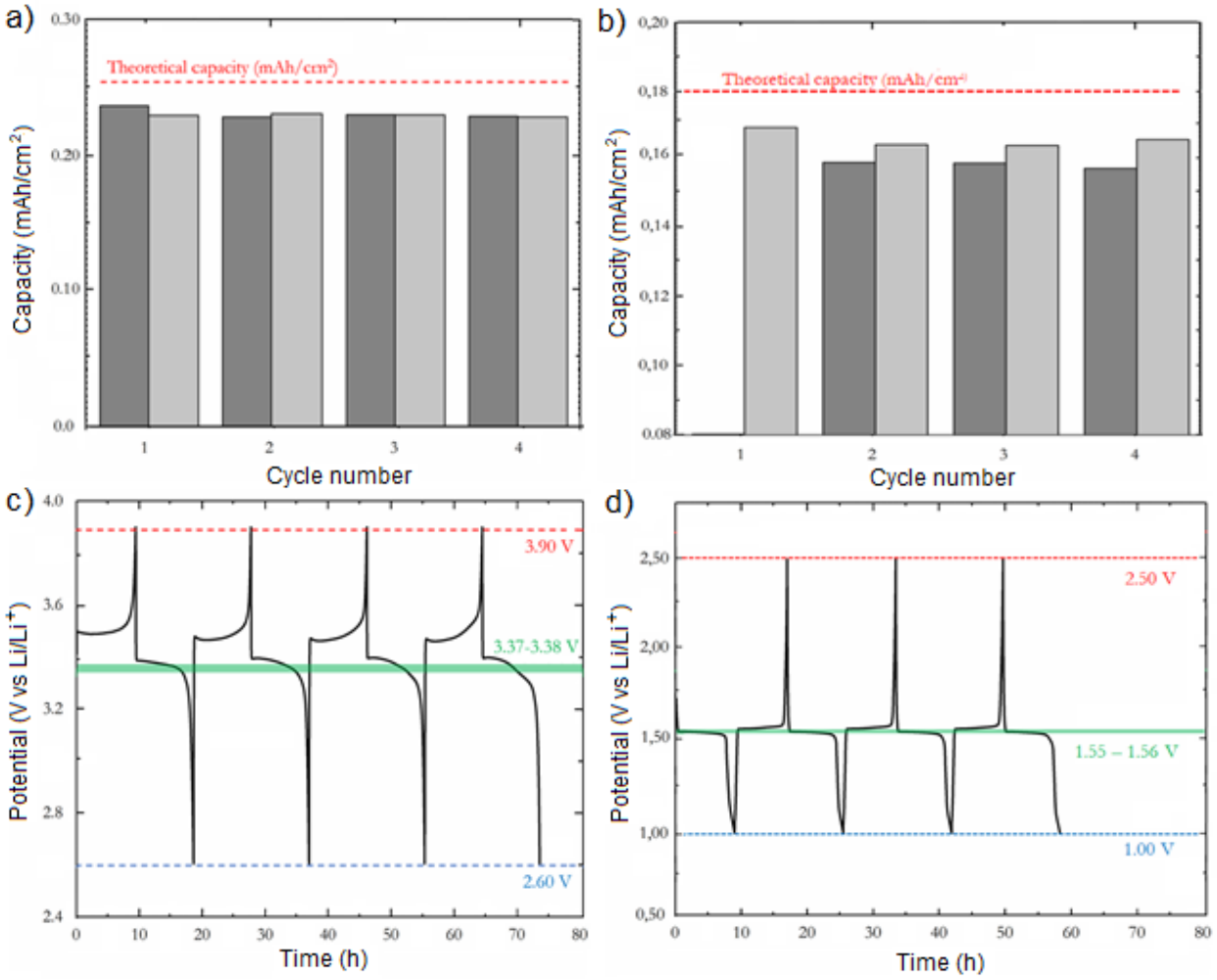

Figure 8. Areal capacity of the a) LFP-A and b) LTO-A in pouch cell configuration; GCD curves of printed reference electrodes, i.e., c) LFP-A and d) LTO-A.

4 Discussion & Conclusion

In summary, SENSIBAT project WP2 investigated different materials for the formulation of inks and pastes to produce printed reference electrodes for Li-ion batteries. To fulfil the printability requirements while maximizing the electrochemical performance of the electrodes, the composition of the ink/pastes has been engineered using PVDF as the binder, a mixture of SLG/FLG and CB as the conductive additives, and LTO and LFP as the active materials. The properties of the produced inks/pastes have been optimized by systematically varying the active materials (LFP/LTO) weight content relatively to the total solid content (from 16% to 80%), while changing the percentage weight (wt%) of the electrically conductive materials relative to the total solid content. This approach has enabled to reach desired electrical resistivity (close to 0.06 Ω·cm), as well as optimal mechanical properties, which in turn resulted in satisfactory paste/ink processability.

Screen printing and Doctor blade techniques have been investigated as suitable printing methods to deposit the produced inks/pastes on the separator. To preliminary investigate the performance of the produced reference electrodes for the subsequent activities of Task 2.4 and Task 2.5, we prepared printed reference electrodes on the porous separators selected by the project (Celgard 2500), Al foil (for LFP-based electrodes) and Cu foil (for LTO-based electrodes) substrates. The SEM imaging confirmed that the material components are well dispersed within the electrode structure without aggregation and provide a conductive network of SLG/FLG and CB that surrounds active material particles.

Cell assemblies using both coin cell and pouch cell configurations have been investigated to test the electrochemical performances of the printed reference electrodes. The printed reference electrodes have shown satisfactory compatibility with commercial LiPF6 EC: DEC (1:1) electrolytes without any deformation and swelling, as already anticipated in Deliverable D2.1. The printed reference electrodes based on 25 wt% of active materials (LFP/LTO) provided the specifications needed by the reference electrodes to enable the following activities of the project. Specific capacity up to 161 mAh g^{-1} have been achieved by the LFP-based reference electrodes and 144 mAh g^{-1} for the LFP-based ones. These values approach the theoretical capacities of the active materials, indicating a quasi-ideal use of the latter. As anticipated in Deliverable D2.1, POL prepared flat-flexible and thin (flat-flex) wiring on printed reference electrode deposited on Celgard 2500. Thus, POL produced 5 cm^2 pouch cells incorporating the as-produced printed reference electrodes, evaluating their effect on the battery cyclability. Both GCD and Li plating/stripping measurements of the batteries including the printed reference electrodes reported a similar behaviour to the one observed for standard, i.e., reference electrode-free, batteries.

The obtained results are promising for the fabrication of printed reference electrodes to meet the challenges ahead for the design of advanced Li-ion batteries with in-situ and in-operando sensing technologies.

5 Risks

The following table reports the risks identified during the Task 2.2's activities, together with the solutions that we successfully proposed to solve them, *de facto* eliminating their occurrence and related effects.

Risk No.	What is the risk	Probability of risk occurrence[1]	Effect of risk[2]	Solutions to overcome the risk
WP2.1	*Unexpected performance of produced reference electrodes*	*1*	*1*	*Changing formulation, using materials from other companies*
WP2.2	*Difficulties with regards to printing of reference electrodes and insufficient adhesion onto the separator*	*2*	*3*	*Changing formulation (increasing binder wt%) and thickness of printed reference electrode on the separator*
WP2.3	*Incompatibility of the produced reference electrodes with the pouch cell assembly process*	*3*	*1*	*Improving the deposition process or changing the formulation*

[1] Probability risk will occur: 1 = high, 2 = medium, 3 = Low

[2] Effect when risk occurs: 1 = high, 2 = medium, 3 = Low

6 References

(1) Zhang, W. J. Structure and Performance of LiFePO4 Cathode Materials: A Review. Journal of Power Sources. 196 (2011) 2962-2970.

(2) Yang, Z.; Choi, D.; Kerisit, S.; Rosso, K. M.; Wang, D.; Zhang, J.; Graff, G.; Liu, J. Nanostructures and Lithium Electrochemical Reactivity of Lithium Titanites and Titanium Oxides: A Review. Journal of Power Sources. 192 (2009) 588-598.

(3) Del Rio Castillo, A. E.; Pellegrini, V.; Ansaldo, A.; Ricciardella, F.; Sun, H.; Marasco, L.; Buha, J.; Dang, Z.; Gagliani, L.; Lago, E.; Curreli, N.; Gentiluomo, S.; Palazon, F.; Prato, M.; Oropesa-Nuñez, R.; Toth, P. S.; Mantero, E.; Crugliano, M.; Gamucci, A.; Tomadin, A.; Polini, M.; Bonaccorso, F. High-Yield Production of 2D Crystals by Wet-Jet Milling. Mater. Horizons 5 (2018) 890–904.

(4) Del Rio-Castillo, A. E.; Ansaldo, A.; Pellegrini, V.; Bonaccorso, F. Exfoliation Materials by Wet-Jet Milling Techniques. WO2017/089987A1, 2017.

(5) Bellani, S.; Martín-García, B.; Oropesa-Nuñez, R.; Romano, V.; Najafi, L.; Demirci, C.; Prato, M.; Del Rio Castillo, A. E.; Marasco, L.; Mantero, E.; D'Angelo, G.; Bonaccorso, F. "Ion Sliding" on Graphene: A Novel Concept to Boost Supercapacitor Performance. Nanoscale Horizons 4 (2019) 1077-1091.

(6) La Mantia, F.; Wessells, C. D.; Deshazer, H. D.; Cui, Y. Reliable Reference Electrodes for Lithium-Ion Batteries. Electrochem. commun. 31 (2013) 141-144.

(7) Ambaye, A. D.; Kefeni, K. K.; Mishra, S. B.; Nxumalo, E. N.; Ntsendwana, B. Recent developments in nanotechnology-based printing electrode systems for electrochemical sensors. Talanta. 225 (2021) 121951

(8) Cherrington, R.; Liang, J.; 2 - Materials and Deposition Processes for Multifunctionality. Design and Manufacture of Plastic Components for Multifunctionality. (2016) 19-51.

(9) Zhang, Y.; Zhu, Y.; Zheng, Sh.; Zhang, L.; Shi, X.; He, J.; Chou, X.; Wu, Zh. Sh. Ink formulation, scalable applications and challenging perspectives of screen printing for emerging printed microelectronics. Journal of Energy Chemistry. 63 (2021) 498-513.2

(10) Ender, M.; Illig J.; Ivers-Tiffée E.; Three-Electrode Setups for Lithium-Ion Batteries I. Fem-Simulation of Different Reference Electrode Designs and Their Implications for Half-Cell Impedance Spectra. J. Electrochem. Soc. 164 (2017) A71-A79

(11) Costard, J.; Ender, M.; Weiss, M.; Ivers-Tiffée E.; Three-Electrode Setups for Lithium-Ion Batteries II. Experimental Study of Different Reference Electrode Designs and Their Implications for Half-Cell Impedance Spectra. J. Electrochem. Soc. 164 (2017) A80-A87.

(12) Xu, P.; Lin, X.; Hu, X.; Cui, X.; Fan, X.; Sun, C.; Xu, X.; Chang, J. K.; Fan, J.; Yuan, R.; Mao, B.; Dong, Q.; Zheng M. High reversible Li plating and stripping by in-situ construction a multifunctional lithium-pinned array. Energy Storage Materials. 28 (2020) 188-195.

(13) Mo, L.; Zheng, H. Solid coated $Li_4Ti_5O_{12}$ (LTO) using polyaniline (PANI) as anode materials for improving thermal safety for lithium ion battery. Energy Reports. 6 (2020) 2913-2918.

(14) Lu, J.; Tian, X.; Zhou, Y.; Zhu, Y.; Tang, Zh.; Ma, B.; Wu, G.; Jiang, T.; Tu, X.; Chen, G. Z. A novel "holey-LFP / graphene / holey-LFP" sandwich nanostructure with significantly improved rate capability for lithium storage. Electrochimica Acta. 320 (2019) 134566

7 Acknowledgement

The author(s) would like to thank the partners in the project for their valuable comments on previous drafts and for performing the review.

Project partners

#	PARTICIPANT SHORT NAME	PARTNER ORGANISATION NAME	COUNTRY
1	IKE	IKERLAN S. COOP.	Spain
2	BDM	BEDIMENSIONAL SPA	Italy
3	POL	POLITECNICO DI TORINO	Italy
4	FHG	FRAUNHOFER GESELLSCHAFT ZUR FOERDERUNG DER ANGEWANDTEN FORSCHUNG E.V.	Germany
5	FM	FLANDERS MAKE VZW	Belgium
6	TUE	TECHNISCHE UNIVERSITEIT EINDHOVEN	The Netherlands
7	NXP NL	NXP SEMICONDUCTORS NETHERLANDS BV	The Netherlands
8	NXP FR	NXP SEMICONDUCTORS FRANCE SAS	France
9	ABEE	AVESTA BATTERY & ENERGY ENGINEERING	Belgium
10	VAR	VARTA MICRO INNOVATION GMBH	Germany
11	AIT	AIT AUSTRIAN INSTITUTE OF TECHNOLOGY GMBH	Austria
12	UNR	UNIRESEARCH BV	The Netherlands

DISCLAIMER/ ACKNOWLEDGMENT

This project has received funding from the European Union's Horizon 2020 research and innovation programme under grant agreement No 957273. The information and views set out in this publication does not necessarily reflect the official opinion of the European Commission. Neither the European Union institutions and bodies nor any person acting on their behalf, may be held responsible for the use which may be made of the information contained therein.